A Supplementary figures

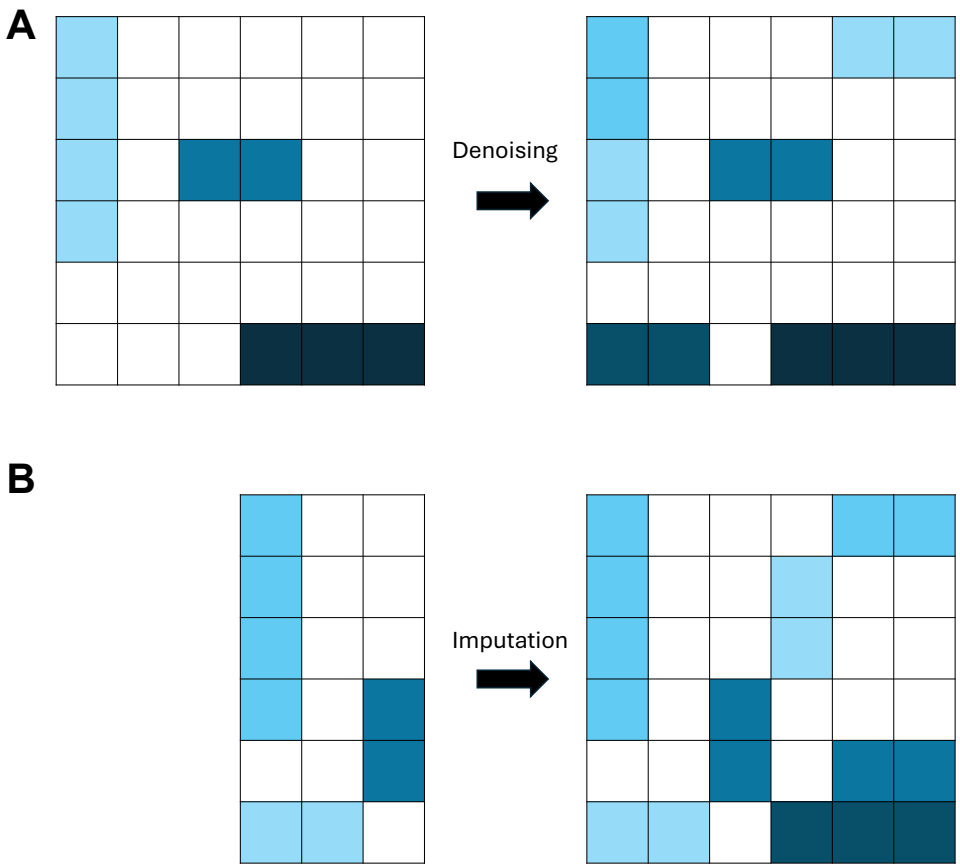

Supplementary Fig. 1 Explanations of imputation and denoising defined in this manuscript. (A) represents the process of data denoising and (B) represents the process of data imputation.

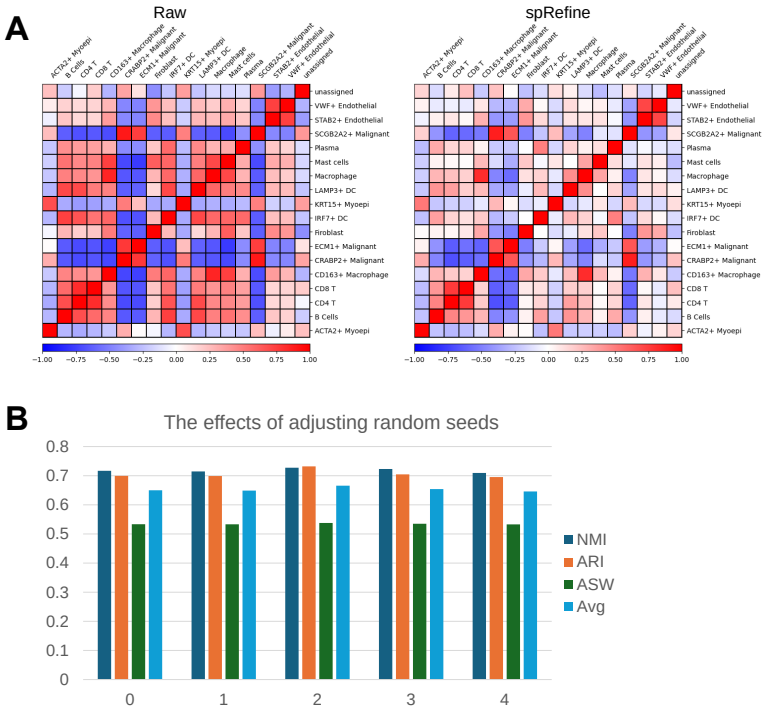

Supplementary Fig. 2 Comparison of cell-type similarity and performance under different random seeds. The dataset analyzed in this figure is xenium_breast. (A) Cell-type-level similarity computed based on gene expression levels. The left panel represents the similarity computed based on the raw profile, while the right panel represents the similarity computed based on the imputed profile. (B) Clustering performance of spRefine across different random seeds.

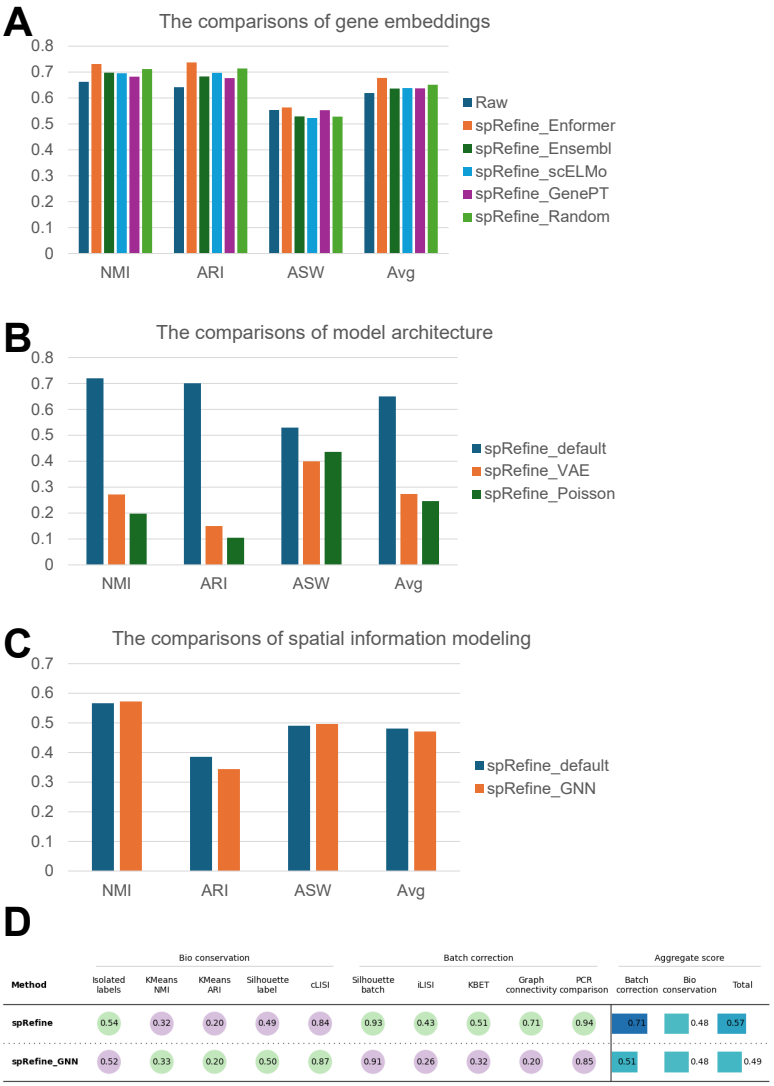

Supplementary Fig. 3 Ablation tests of spRefine. (A) Clustering performance of spRefine with gene embeddings from different sources based on the breast_xenium dataset. (B) Clustering performance of spRefine with different model architectures based on the breast_xenium dataset. (C) Clustering performances of spRefine with spatial modeling approaches based on the brain_xenium dataset. (D) Comparison of batch effect correction performances between spRefine with and without GNN encoder.

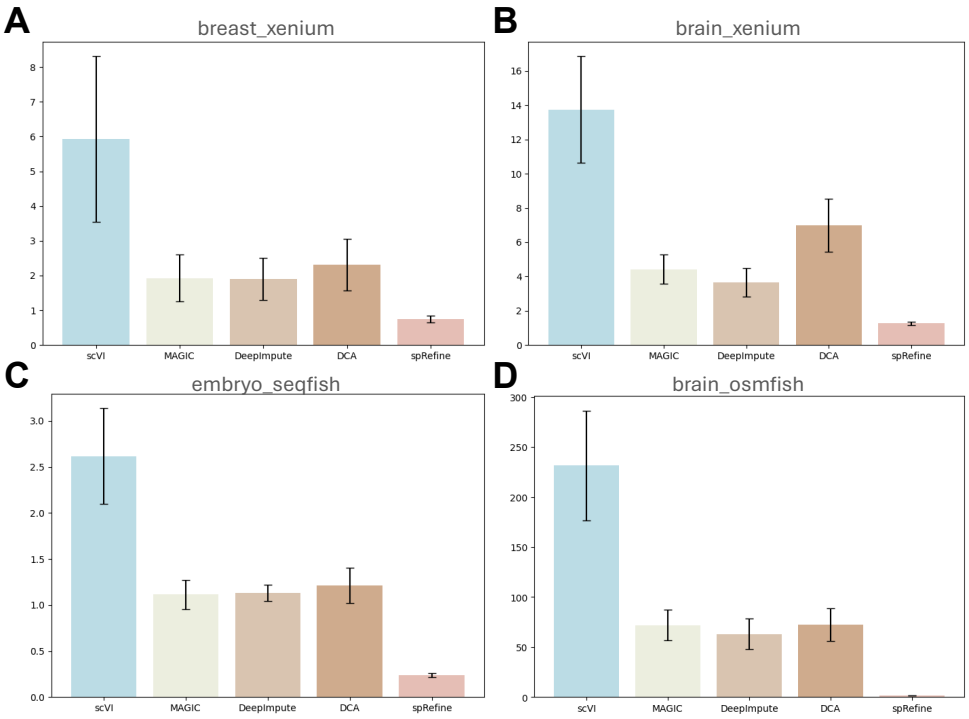

Supplementary Fig. 4 Comparisons of data denoising based on different methods. (A) MSE results based on the breast_xenium dataset. (B) MSE results based on the brain_xenium dataset. (C) MSE results based on the embryo_seqfish dataset. (D) MSE results based on the brain_osmfish dataset.

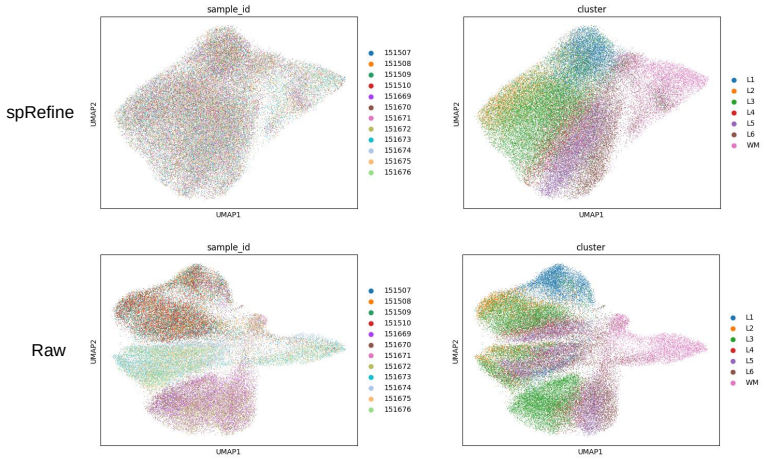

Supplementary Fig. 5 UMAP visualization of gene expression profiles before and after denoising+batch effect correction. These figures are colored by batch labels (sample_id) or cell types (cluster).

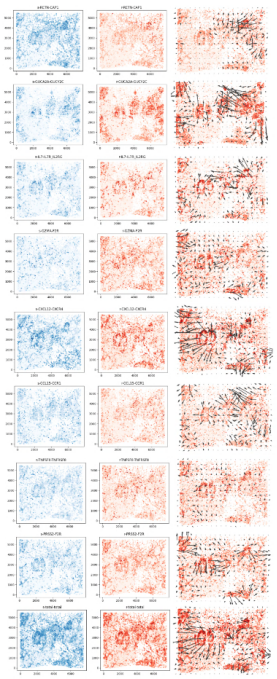

Supplementary Fig. 6 The first part of measured CCCs. Each line contains three panels, including sender strength, receiver strength, and signal directions.

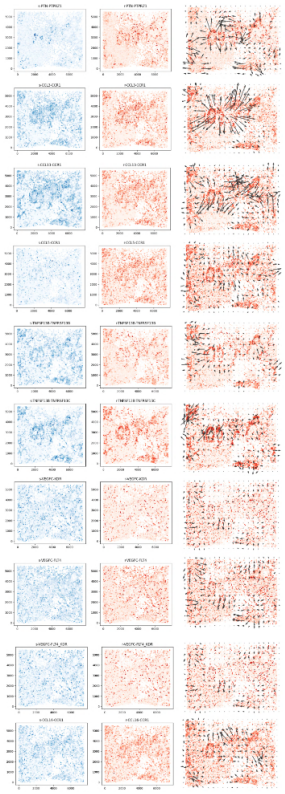

Supplementary Fig. 7 The second part of measured CCCs. Each line contains three panels, including sender strength, receiver strength, and signal directions.

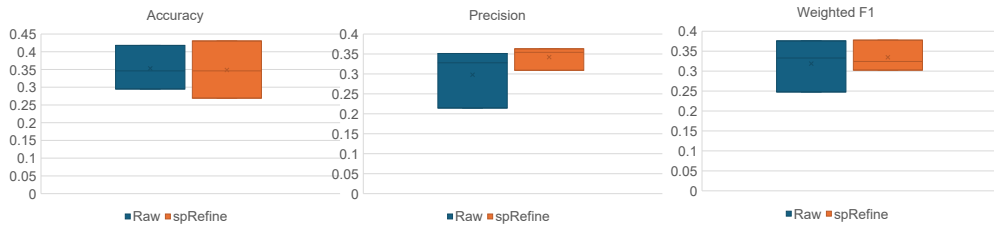

Supplementary Fig. 8 Comparison of disease-state prediction performances between the raw and imputed profiles by spRefine. Here we selected 10% of the cells in the original data to implement the training.

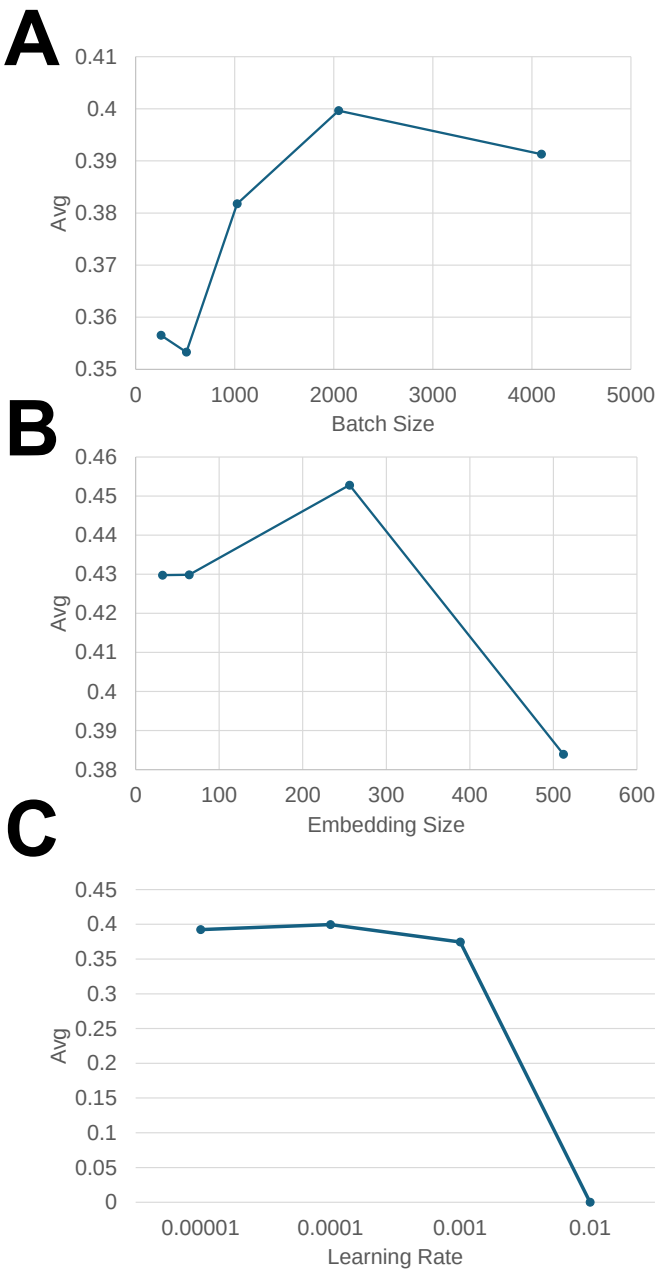

Supplementary Fig. 9 The comparisons of clustering performances based on different hyper parameters. (A) Model performances under different batch sizes. (B) Model performances under different embedding sizes. (C) Model performances under different learning rates.